

The irreversible thermodynamic's theorem of minimum entropy production applied to the laminar and the turbulent Couette flow

Hans Paul Drescher

Galileo-Allee 8, D-52457 Aldenhoven, Germany

hanspaul.drescher@budi.de

November 2018

Abstract

Analyzing thermodynamic non-equilibrium processes, like the laminar and turbulent fluid flow, the dissipation is a key parameter with a characteristic minimum condition. That is applied to characterize laminar and turbulent behaviour of the Couette flow, including its transition in both directions. The Couette flow is chosen as the only flow form with constant shear stress over the flow profile, being laminar, turbulent or both. The local dissipation defines quantitative and stable criteria for the transition and the existence of turbulence. There are basic results: The Navier Stokes equations cannot describe the experimental flow profiles of the turbulent Couette flow. But they are used to quantify the dissipation of turbulent fluctuation. The dissipation minimum requires turbulent structures reaching maximum macroscopic dimensions, describing turbulence as a "non-local" phenomenon. At the transition the Couette flow profiles and the shear stress change by a factor $\cong 5$ due to a change of the "apparent" turbulent viscosity by a calculated factor $\cong 27$. The resulting difference of the laminar and the turbulent profiles results in two different Reynolds numbers and different loci of transition, which are identified by calculation.

Keywords:

Turbulence, transition, minimum dissipation

Table of Contents

	Page
1. Introduction	1
1.1 The statement	1
1.2 The minimum theorem of dissipation/entropy production	2
2. Results for the Couette Flow	4
2.1 The laminar Couette flow	4
2.2 The turbulent Couette flow	6
3. Additional fluid flow mechanism, nonlocal and delayed dissipation	8
3.1 Turbulent flow elements	8
3.2 Maximum turbulent dimensions	12
3.3 Turbulent fluctuation and dissipation	13
3.4 Comparison with Prandtl's turbulent mixing length hypothesis	16
3.5 A "local" Reynolds number	18
4. Laminar and turbulent flow, theory and experiment	20
4.1 Macroscopic turbulent dimensions	20
4.2 Difference of laminar / turbulent flow profiles	25
4.3 Hysteresis of the laminar-turbulent-laminar transition	27
4.4 Smooth local transition ("law of wall")	32
5. Numerical calculations	37
5.1 A 1-dimensional equation for a turbulent profile	37
5.2 Numerical examples for Couette and pipe flow	40
6. Summary	44
7. Acknowledgments	45

Literature, special parameters

1. Introduction

1.1 The statement

The entropy production/dissipation is an important parameter to analyze and describe physical non-equilibrium processes. In this paper that will be used to explain the existence of and the transition to turbulence and back. The thermodynamics of irreversible (non-equilibrium) processes give the background.

Since the identification of “turbulence” by Reynolds in 1883 the idea was that an “instability” of the Navier-Stokes equations explains the phenomenon of the transition laminar-to-turbulent. This paper explains turbulence as a stable process with stable limits between turbulent and laminar zones, being well defined by a minimum dissipation requirement.

That is not common in the theories of fluid dynamics. J. Meixner, one of the pioneers of the thermodynamics of irreversible processes /1/, summarizes the deficits of the theories of fluid flow: „Klassische Lehrbücher der theoretischen Physik behandeln die Hydro- und Aerodynamik in der Regel ohne auf die thermischen Effekte einzugehen ... Man findet dies nicht in einem klassischen Lehrbuch der theoretischen Physik, obwohl es ein charakteristisches und interessantes und technisch wichtiges Beispiel der Kontinuums-Physik ist.“ /2/

The laminar/turbulent flow is a dissipative, meaning an irreversible thermodynamic process requiring a continuous input of mechanical energy. With the changeover laminar-to-turbulent, the flow resistance of the experiment increases spontaneously by a factor 3 – 10, thereby the dissipation. The mechanical drive of the experiment has to be geared up by that magnitude.

“Instability” does not explain that increase of dissipation. Th. v. Kármán remembers early discussions with A. Sommerfeld, one of the pioneers of “hydrodynamic instability”, resulting in a very critical remark: “Der Bedeutung der Turbulenz war er (Sommerfeld) nicht nähergekommen!“ /19/

The calculations of this paper have been made for the Couette flow, which allows a simple and straightforward calculation of the dissipation and the shear stress. The “principle of least dissipation” is fulfilled for the laminar, linear Couette profile. Any other non-laminar, non-linear Navier-Stokes solution for any other Couette profile would violate that “principle”. That consequence is remarkable when discussing turbulence to be described by the Navier-Stokes equations.

1.2 The minimum theorem of dissipation/entropy production

Helmholtz and Rayleigh describe a minimum dissipation theorem based on the Navier-Stokes equations. It states that the flow of an incompressible fluid – at any time and any position – has minimum conceivable dissipation /3/.

Equivalent but more common is the theorem of minimum entropy production of the thermodynamics of irreversible processes. It states that in stationary thermodynamic systems all existing thermodynamic processes proceed in a manner that the entropy production becomes minimal /4/.

The theory of irreversible thermodynamic processes is associated with the famous names Onsager (Nobel Prize 1966), Casimir, Eckart, Meixner, de Groot, Prigogine (Nobel Prize 1977). The minimum requirement is mentioned as “Prigogine-Prinzip” in the German Brockhaus Enzyklopädie /5/ and as “Rayleigh-Onsager principle of least dissipation or principle of minimum entropy production” in the British Encyclopaedia Britannica /1/.

Klimontovich /8/ verifies the minimum condition for turbulent shear flows.

Malkus and Busse /7/ conclude that dissipation reaches its maximum in turbulent flow conditions: “The realized turbulent shear flow represents the flow with maximum dissipation at a given Reynolds number among all possible solutions of the Navier-Stokes equations of motion.” This statement fully contradicts the theorems above.

Classical fluid theories recognise the concepts of corpuscular theory and continuum theory. A fluid can also be considered as a system of discrete mass points and its mechanical behavior can be dealt with by methods of the mechanics of point systems. In contrast, the continuum theory uses certain “material constants” for characterising the material.

Classical, theoretical mechanics are equipped with a variety of tools for describing extreme minimum properties of such mechanical point systems. In 1747 Maupertuis developed the “Prinzip der kleinsten Wirkung”, which was later justified more rigorously by his colleagues Euler and Lagrange at the Prussian Academy of Sciences in Berlin and by Hamilton. It is supplemented by Gauss’s “Prinzip des kleinsten Zwanges” (Gauss 1829, Jacobi 1842) /11/ /12/.

It is indisputable that both model approaches must not lead to different physical conclusions. Information on this aspect is rare in the literature. G.E.A. Meier points out that “the kinematic component (Note: “mass points” from a mechanics perspective) of non-steady motion play a much greater role than one could have previously supposed based on the closed treatment of the corresponding systems of equations” /13/. Behind Prandtl’s mixing length hypothesis “a certain analogy to the kinetic theory of gases” can be seen as mentioned by Schlichting /9/. Further mechanisms are discussed by Durst /10/ and Nehring /14/.

A “corpuscular” character of fluid flow is an important argument in the later chapters.

2. Results for the Couette Flow

2.1 The laminar Couette flow

For a fluid flow between parallel walls – the Couette flow in Fig. 1 – the Navier-Stokes equations give a simple, one-dimensional, linear, stationary velocity profile.

The shear stress τ is constant across the profile, simplified to

$$\tau = \mu \frac{du}{dy} = \text{const.} \quad (1)$$

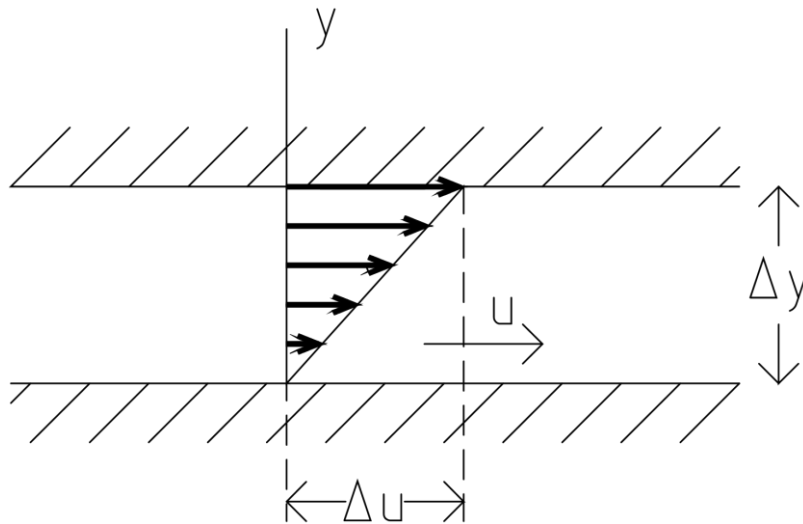


Fig. 1: Plane laminar Couette flow

A constant mechanical power input $\tau \Delta u$ is applied by the walls of the test equipment and is converted into heat within the fluid. This is a dissipative and therefore irreversible thermodynamical process.

The dissipation per volume element \dot{E} is calculated

$$\dot{E} = \tau \frac{du}{dy} = \mu \left(\frac{du}{dy} \right)^2 \quad (2)$$

The dissipation increases quadratically with the shear rate. The linear flow profile includes the minimum conceivable dissipation.

This dissipation has to take place

- infinitesimally locally,
- completely,
- without delay.

If there is even the slightest doubt about this and under such conditions a “delayed” energy dissipation is present, the energy balance is unclosed.

The literature of “instability” gives the result that the laminar Couette flow is stable for all conditions and all Reynolds numbers /9/. (An advanced non-linear stability analysis could lead to an instability of the Couette flow solution /18/). The minimum dissipation theorem of Rayleigh and Helmholtz gives the result that any solution of the Navier-Stokes equations gives a minimum conceivable dissipation /3/.

Consequence:

- The Navier-Stokes equations will not describe any non-laminar Couette flow.

2.2 The turbulent Couette flow

With higher Reynolds numbers the Couette flow is turbulent. Fig. 2 shows different flow profiles.

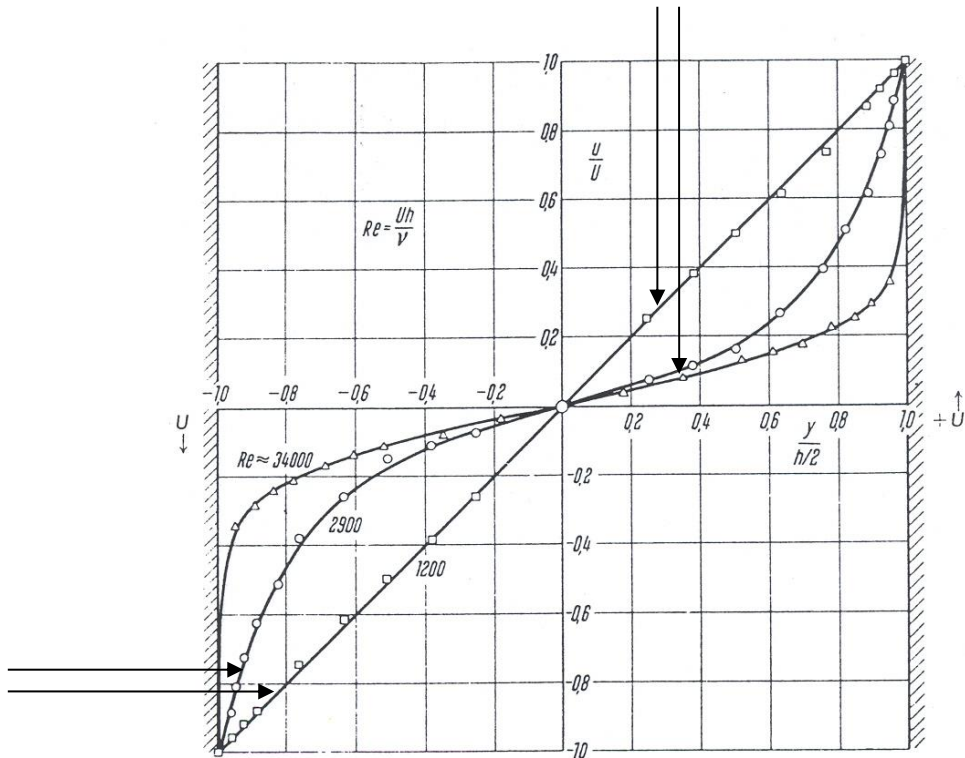


Fig. 2: Velocity profile of the Couette flow between two parallel plane opposing walls /27/

The flow profiles found in the turbulent experiment at higher Reynolds numbers give a higher dissipation than the linear profile in Fig. 1.

The Couette flow is the only flow form with a constant shear stress over the complete flow profile, being laminar, turbulent or both.

The constant shear stress is simplified to Eq. 1, the dissipation per volume element to Eq. 2. The 3-dimensional definition is

$$\tau_{ij} = \mu \left(\frac{\partial \mu_j}{\partial x_i} + \frac{\partial \mu_i}{\partial x_j} \right)$$

The shear stress τ (or τ_{ij}) is proportional to the gradient. With $\tau = const.$ for the Couette flow the gradient according to Navier Stokes has also to be constant – and is not.

The turbulent Couette flow profiles in Fig. 2 require a non-linear relation between gradient $\frac{du}{dy}$ and shear stress τ , which is not given by the constant value of the viscosity μ .

Consequence:

- The Navier Stokes equations cannot describe the experimental flow profile of the turbulent Couette flow.

The “apparent” turbulent viscosity μ_{turb} calculated in Chapt. 3 (see Eq. 10, 18, 19) shows that non-linearity, required for the Couette flow, similar to the non-linear definition in Prandtl’s mixing length hypothesis (Chapt. 3.4).

3. Additional fluid flow mechanism, nonlocal and delayed dissipation

3.1 Turbulent flow elements

We consider fluid dynamic mechanisms additional to the Navier-Stokes equations with the focus on processes with the possibility of delayed and nonlocal dissipation.

There is an interesting “fundamental paradox” of turbulence modeling between the local character of the partial differential equations strongly favored by CFD methods and the nonlocal physical nature of turbulence”, mentioned by Ph. R. Spalart /16/.

The focus of the following chapters is not a highly sophisticated theory. Turbulence, especially its transition, is a rude process, easily to be observed by drastic changes of the physical flow parameters. Every pilot of an aircraft and every sailor can tell stories about that. A simplified physical description of the phenomenons should be possible.

The following chapters make use of simplifications:

- Couette flow
- Laminar zones described by the Navier Stokes equations
- Turbulence zones described under the assumption of nonlocal momentum exchange and “delayed” dissipation due to a “corpuscular behaviour”
- The dissipation of turbulent fluctuation is calculated by Taylor’s theory based on the Navier Stokes equations
- Transition between the zones defined by the condition of minimum local dissipation

The results explain an increase of the flow resistance (factor >5), of the gradients of the flow profile near the wall (factor >5) and of the apparent “viscosity” (factor >27) in spite of the local minimum dissipation of the turbulent zones. They also explain two different Reynolds numbers for the two directions of transition. The results are compared with the empirical values in Ch. 4.1-4.4.

We consider the plane Couette flow, Fig. 3. Contrary to the laminar Couette flow in Fig. 1, the flow profile is not linear, but S-shaped in advance of later results. In that we consider a volume having a dimension D at a sufficient distance from the walls. The dimension D is macroscopic, but unknown in the moment.

We assume that a momentum exchange takes place in this volume element, but that any dissipation takes place with a delay.

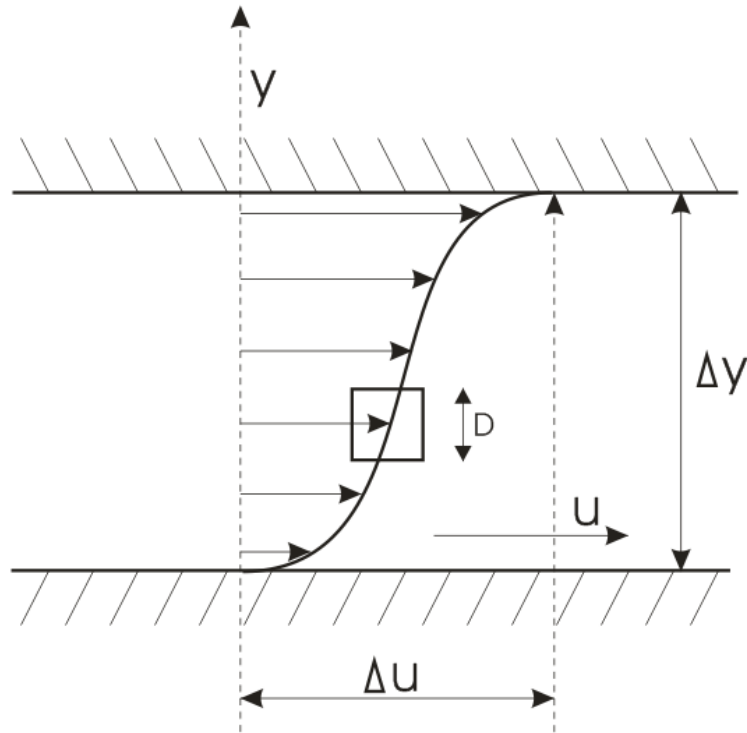


Fig. 3: Plane Couette flow

The origin of coordinates is assumed to be in the centre of the D-element (Fig. 4). With a linear profile $\frac{du}{dy} = \text{const.}$ the kinetic energy E_{Kin} of all mass points of the D-element is

$$E_{Kin} = D^2 \int_{-D/2}^{D/2} \frac{1}{2} \rho \left(\frac{du}{dy} y \right)^2 dy = \frac{1}{24} \rho \left(\frac{du}{dy} \right)^2 D^5 \quad (6)$$

After the momentum exchange, all mass points may possess equal kinetic energy. So the resulting mean value of the velocity given by $|V_{qu}|$ is

$$\frac{1}{2} \rho D^3 V_{qu}^2 = \frac{1}{24} \rho \left(\frac{du}{dy} \right)^2 D^5 \quad (7)$$

$$|V_{qu}| = \frac{1}{\sqrt{12}} \frac{du}{dy} D$$

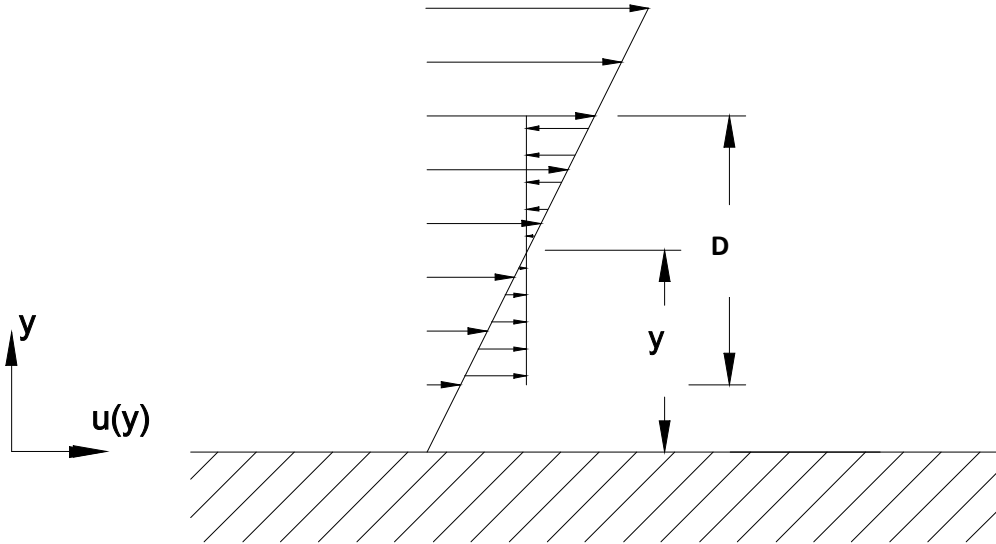


Fig. 4: Momentum exchange within the D-element

This way, the averaged total momentum of the upper and lower half spaces is adapted.

We now determine the momentum exchange Δp on surface $y = \text{const.}$ in the centre of the D-element as a measure for the “apparent” shear stress τ .

$$\begin{aligned}
 \Delta p &= \int_{-D/2}^{D/2} |\rho u(y)| dy \\
 &= 2 \int_0^{D/2} \rho \frac{du}{dy} y dy \\
 &= \frac{1}{4} \rho \frac{du}{dy} D^2
 \end{aligned}$$

We consider that exchange to be complete after the time ΔT when all mass elements of the D-volume have moved at their average velocity component along the distance $\frac{D}{2}$.

The average velocity component of all mass elements per mean coordinates in $\frac{V_{qu}}{6}$, this lateral to the mean flow through the plane $y = 0$ is $\frac{V_{qu}}{3}$. Thus $\Delta T = \frac{D}{2} \cdot \frac{1}{\frac{1}{3} V_{qu}}$

Further calculation leads to the apparent “shear stress” τ

$$\tau = \frac{\Delta p}{\Delta T} \quad (8)$$

$$\tau = \frac{1}{12\sqrt{3}} \rho \left(\frac{du}{dy} \right)^2 D^2$$

We verify this result by adopting a simple approach, i.e. the “analogy to the kinetic theory of gases” described in Prandtl’s mixing length hypothesis [9/ /20/]. According to the kinetic theory of gases the viscosity is

$$\mu = \frac{1}{3} \rho l \bar{c} \quad (9)$$

where ρ is the density, l the mean free length, and \bar{c} the mean velocity of gas molecules.

Replacing the mean free distance l with $\frac{D}{2}$ and the mean molecular velocity \bar{c} with V_{qu} , the apparent “viscosity” μ_t is given by

$$\begin{aligned} \mu_t &= \frac{1}{3} \rho \frac{D}{2} V_{qu} \\ &= \frac{1}{12\sqrt{3}} \rho \frac{du}{dy} D^2 \end{aligned} \quad (10)$$

and

$$\begin{aligned} \tau_t &= \mu_t \frac{du}{dy} \\ &= \frac{1}{12\sqrt{3}} \rho \left(\frac{du}{dy} \right)^2 D^2 \end{aligned}$$

which confirms the mentioned result.

3.2 Maximum turbulent dimensions

The question arises on the possible quantitative D values. For this the condition of minimum dissipation gives a surprising result.

The local dissipation \dot{E} can be expressed as

$$\dot{E} = \tau \frac{du}{dy}$$

or, with τ according to Eq. 8,

$$\dot{E} = \sim \left(\frac{du}{dy}\right)^3 D^2$$

For any Couette flow profile the shear stress is constant

$$\tau = \sim D^2 \left(\frac{du}{dy}\right)^2 = \text{const.}$$

or

$$\frac{du}{dy} \sim \frac{1}{D} \tag{11}$$

and thus

$$\dot{E} \sim \frac{1}{D} \tag{12}$$

The dissipation decreases as D increases. For the dissipation to be at its minimum, D has to assume maximum possible values – characterizing the dissipation \dot{E} as “nonlocal”.

The maximum possible D-values are limited by the fact that the D-volume must not approach the boundary conditions (walls). From the condition of continuity and the assumed incompressibility of the fluid near the wall it follows that volume is displaced by transverse flow at a velocity which becomes higher as the distance from the wall decreases and D increases. Excessive dimensions and too great a proximity to the wall would contradict the definition of the D-element (undisturbed momentum exchange).

The proximity to the wall is a limiting factor for a maximum value D. The approach below is chosen

$$D = \alpha y \quad y = \text{wall distance} \quad (12a)$$

The approach with a scaling factor α

$$\alpha = 1.33$$

gives a good idea of a maximum conceivable dimension of a D-volume with a momentum exchange that is still “undisturbed” despite its proximity to the wall (Fig. 4).

3.3 Turbulent fluctuation and dissipation

To analyse the dissipation we use the well-known approach of Taylor (1935) for isotropic, turbulent fluctuations. We follow the description given by Schlichting, Landau, Prandtl /9,20,21/.

The quantities relevant to turbulent flows, e.g. velocity u , are subdivided into a mean value \bar{u} and a superimposed fluctuation u'

$$u_i = \bar{u}_i + u'_i \quad i = 1,2,3 \quad (13)$$

The local dissipation \dot{E} is calculated from the Navier-Stokes equations

$$\dot{E} = \mu \left[2 \left(\frac{\partial u_1}{\partial x_1} \right)^2 + 2 \left(\frac{\partial u_2}{\partial x_2} \right)^2 + 2 \left(\frac{\partial u_3}{\partial x_3} \right)^2 + \left(\frac{\partial u_2}{\partial x_1} + \frac{\partial u_1}{\partial x_2} \right)^2 + \left(\frac{\partial u_3}{\partial x_2} + \frac{\partial u_2}{\partial x_3} \right)^2 + \left(\frac{\partial u_1}{\partial x_3} + \frac{\partial u_3}{\partial x_1} \right)^2 - \frac{2}{3} \left(\frac{\partial u_1}{\partial x_1} + \frac{\partial u_2}{\partial x_1} + \frac{\partial u_3}{\partial x_1} \right)^2 \right] \quad (14)$$

If one introduces the velocity according to equation (13) into the term for energy dissipation equation 14, one obtains a proportion which depends on the gradient of the average velocity \bar{u} (usually called “direct dissipation”) and a proportion \dot{E}'_t , which depends on the gradients of the fluctuation movement. The latter is simplified after averaging to

$$\dot{E} = \mu \left[2 \overline{\left(\frac{\partial w_1}{\partial x_1} \right)^2} + 2 \overline{\left(\frac{\partial w_2}{\partial x_2} \right)^2} + 2 \overline{\left(\frac{\partial w_3}{\partial x_3} \right)^2} + \overline{\left(\frac{\partial w_1}{\partial x_2} + \frac{\partial w_2}{\partial x_1} \right)^2} + \overline{\left(\frac{\partial w_1}{\partial x_3} + \frac{\partial w_3}{\partial x_1} \right)^2} + \overline{\left(\frac{\partial w_2}{\partial x_3} + \frac{\partial w_3}{\partial x_2} \right)^2} \right] \quad (15)$$

Taylor's further analysis gives

$$\dot{E}_t = 15 \mu \overline{\left(\frac{\partial u'_i}{\partial x_k}\right)^2} \quad (\text{for one arbitrary combination of } i, k) \quad (16)$$

With the approach of Taylor we make use of the Navier-Stokes equations which are criticized in this paper. At the end of this chapter a local Reynolds number is defined, with "critical" values defining a local condition for the existence of turbulent flow. For the fluctuations u'_i in Eq. 13 these local values are by a factor 20-100 below that "critical" value.

Here an assumption of the mean fluctuation in Eq. 16 with the lowest possible dissipation is required. This is represented in a simplified manner in Fig. 5 as a conceivable distribution of variation component u'_y . The zigzag shape of the profile was chosen because $\frac{\partial u'_y}{\partial x}$ is used in square terms in Eq. 16 and any other shape would result in higher values of dissipation \dot{E}_t . The influence of that simplification on the factor 27 in Eq. 19 can be discussed.

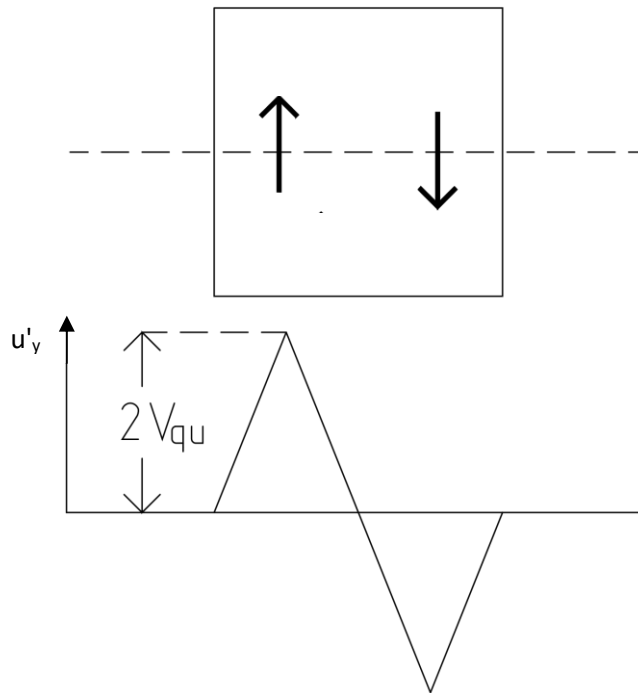


Fig. 5: Assumption of fluctuation in one third of the D^3 -volume

For the third part of the D³-volume outlined in Fig. 10 thus we see

$$\left| \frac{\partial u_y}{\partial x} \right| = 8 \frac{V_{qu}}{D}$$

and relative to the entire D-volume

$$\left(\overline{\frac{\partial u_y}{\partial x}} \right)^2 = \frac{1}{3} \cdot 64 \cdot \frac{V_{qu}^2}{D^2}$$

When applied to Eq. 16 the expression is

$$\dot{E}_t = 320 \mu \frac{V_{qu}^2}{D^2} \quad (17)$$

\dot{E}_t in Eq. 17 defines the minimum conceivable value of dissipation.

The input of mechanical power introduced into the D-volume $\tau_t \frac{du}{dy}$ (τ_t according to Eq. 8) has to be greater than the (minimum conceivable) turbulent dissipation \dot{E}_t according to Eq. 17. Combined reading Eq. 8 for τ_t and Eq. 7 for V_{qu} leads to

$$\frac{1}{12\sqrt{3}} \rho \left(\frac{du}{dy} \right)^3 D^2 \geq \frac{320}{12} \mu \left(\frac{du}{dy} \right)^2 \quad (18)$$

or, after division by $\left(\frac{du}{dy} \right)^2$ with Eq. 10,

$$" \mu_{\text{turb}} " \geq 27\mu \quad (19)$$

μ_{turb} is enclosed in parentheses to remind the reader that the viscosity is an "apparent" one.

The result of this analysis is that turbulence is possible only if the "apparent" turbulent viscosity resulting from the macroscopic fluctuation is at least 27 times greater than the Newton viscosity μ .

The Couette flow is the flow experiment with a constant sheer stress over the profile. So the flow profile at the locus of turbulent transition has to be much flatter than before the transition (thereby reducing the dissipation in spite of increasing μ_{turb}).

3.4 Comparison with Prandtl's turbulent mixing length hypothesis

Prandtl's mixing length hypothesis is discussed to be an important step in explaining turbulent flow behavior. The hypothesis has no approach by the Navier-Stokes equations.

Prandtl assumes that in a turbulent flow packets of fluid have an independent motion and move both longitudinally and laterally over an average distance l , under conservation of their momentum. The resulting fluctuations are explained by fluid packets of different velocities encountering each other. Prandtl describes the mixing length by adopting the "analogy to the kinetic theory of gases" /9/ /20/.

A further result of Prandtl and v. Kármán is the logarithmic shape of the turbulent flow profile. This is admired as an important and classical result. Marusic emphasizes: "The beauty of this classical result is its simplicity particularly given the complexity of the multi scale non-linear problem at hand" /22/. The theorem of minimum dissipation gives the same result by a very simple approach (see Eq. 11).

The turbulent shear stress is calculated as

$$\tau = \rho l^2 \left(\frac{du}{dy} \right)^2 \quad (20)$$

Prandtl's theory makes no statement on the size and form of the fluid packets. The dimension of the mixing length l is determined empirically from the flow profile of the experiment. It is interesting to compare the results for Eq. 22 with the numerical results of Eq. 8 in the preceding chapters.

Some differences of Prandtl's mixing length hypotheses are a noteworthy.

- The mixing length is defined exclusively as a locus function of the wall distance. This is questionable because every location of the flow profile is reached and influenced by mixing lengths of different sizes and from all directions.
- The mixing length gives no indication of the thickness of the laminar boundary layer near the wall and of the transition to turbulence.
- The definition of the mixing length is an exclusively empirical operand rather than a phenomenological measure for the range of turbulent mixing motion. Prandtl's formulation lacks a factor 1/3 if one considers l the physical measure for a "range" of convective momentum exchange (this lack is not important for the hypothesis because l is determined empirically anyway) /10/. Physically this "range" is greater by a factor $\sqrt{3}$ than the "mixing lengths", the term commonly used in the literature. The empirical results lead to $l = 0,4 y$ near the wall, decreasing to $l = 0,14 y$ near the center of a pipe flow.

For the comparison we substitute in Eq. 20 $l = 0,4 y$ decreasing to $l = 0,14 y$ ($y =$ wall distance) and in Eq. 8 $D = \frac{3}{4}y$. By this

Prandtl's Eq. 22 becomes

$$\tau = \rho \cdot 0,16 \cdot y^2 \left(\frac{du}{dy} \right)^2 \text{ near the wall}$$

$$\tau = \rho \cdot 0,02 \cdot y^2 \left(\frac{du}{dy} \right)^2 \text{ near the center of the pipe}$$

and Eq. 8 becomes

$$\tau = \rho \cdot 0,085 \cdot y^2 \left(\frac{du}{dy} \right)^2$$

Both equations can be compared in spite of the completely different origin and background, if the difference between pipe flow and Couette flow is taken into account.

3.5 A “local” Reynolds number

The Reynolds number has been the focus of a lot of dimensional analyses.

We add a further dimensional discussion. The relation in Eq. 18 becomes dimensionless by dividing by $\mu \left(\frac{du}{dy}\right)^2$

$$\frac{\left(\frac{du}{dy} \cdot D\right) \cdot D}{\frac{\mu}{\rho}} \geq 555 \quad (21)$$

With $\frac{du}{dy} \cdot D$ as “characteristic velocity” and D as “characteristic length” this equation takes the form of a Reynolds number. This is now a locus function defining a local minimum condition for the existence of turbulent flow

$$Re_{D,krit} = f(D) \geq 555 \quad (21a)$$

With $D = \frac{4}{3} y$ in Eq. 12a we substitute Eq. 21.

$$\frac{\left(\frac{du}{dy} \cdot y\right) \cdot y}{\frac{\mu}{\rho}} \geq 310 \quad (22)$$

We further substitute

$$Re_{local} = \frac{\rho y^2 \frac{du}{dy}(y)}{\mu} \quad (22a)$$

with the wall distance y and the gradient $\frac{du}{dy}(y)$. Eq. 22a is influenced by the wall distance and by the form of the flow profile, being laminar or turbulent.

The denominator in Eq. 22a is equivalent to the “apparent” turbulent “viscosity” in Eq. 10 (after including a factor) and equivalent to Prandtl’s hypothesis (after quantifying the mixing length $l = 0,4 \cdot y$, the empirical value near the wall /9/).

Prandtl's theory gives no indication for the existence of turbulence. If turbulence exists at sufficient high gradients $\frac{du}{dy}$ and sufficient high wall distance y , the value of Re_{local} is equivalent to a value of the ratio $Re_{local} = \frac{\mu_{turb}}{\mu}$ (after including the factor).

4. Laminar and turbulent flow, theory and experiment

4.1 Macroscopic turbulent dimensions

The dissipation decreases as D increases. For the local dissipation to be at its minimum, D has to assume maximum possible values. An important consequence of this statement is that the turbulent motion pattern with maximum possible characteristic dimensions is a “normal case”.

The conclusion that the characteristic dimensions of turbulence assume maximum values results in a change in perspective: Turbulence is not the result of “unstable” laminar motion but the normal condition or, as argued by Klimontovich /8/ focusing the minimum condition, “turbulent flow has a greater degree of order than laminar flow”. Marusic et al. /22/ mention “many unanswered questions in respect of very large scale motions (VLSMs)” or “superstructures”.

The question arises how far this can be observed in the free atmosphere. The spatial extent and the temporal course of the occurring flow events are of particular interest. Based on the considerations in Chapter 3, we expect turbulence elements of a size >100 m and exchange times of several minutes.

For such an observation, the visible part of cooling tower- and chimney plumes can be used. Such a plume is saturated with water vapour and becomes visible – similar to a cloud – through condensed water droplets. At a certain distance from the source, it can usually be observed that the plume “dissolves”. This “dissolution” is mainly caused by turbulent mass and heat exchange. Large-scale exchange processes must therefore become visible on large structures of the plume image. The area where the plume has dissolved and only a few shreds remain is particularly interesting. Some of the distances between them show a very distinctive scaling.

Thermal and meteorological effects are superimposed on these exchange processes. An unstable atmospheric stratification amplifies the turbulent exchange or superimposes it. A stable atmospheric stratification or even an inversion impedes the turbulent vertical exchange. The temperature and the evaporation energy of the visible cloud influence the atmospheric layering itself.

The interest remains for weather conditions with a medium dry atmosphere, medium wind conditions and a largely neutral atmospheric layering. For this we expect scaling effects of size $\frac{D}{2}$, i. e. about $\frac{2}{3}$ y.

Fig. 6 shows observations using the Weisweiler power plant as an example. The originally closed cloud image of the cooling tower plume breaks up into clearly identifiable individual cloud areas, whose distance is roughly comparable to the distance to the ground. The calculated "time" for the turbulent exchange is approx. 2.5 min. with the given wind speed.



Fig. 6: Weisweiler power plant, 12/26/2009, 9.26 Uhr (1 min. time difference)
temperature 4 °C, wind 230 °/7-10 m/s

Depending on the weather conditions, a large power plant shows a very impressive cooling tower plume. This is distracting from the fact that the main focus should be on the area where the plume almost completely dissolves.

A smaller chimney plume is shown in Fig. 7 of the Jülich sugar refinery. On the right side of the photos one can still see just visible shreds of plume (marked with black arrows). Their distance confirms the estimated scaling. In the left part of the photo, the extensive breaking up of the chimney plume begins.

One can practically always find such a qualitative scaling, if the turbulence structures of a cooling tower or chimney plume become visible with suitable atmospheric conditions. The turbulent mixing movement thus involves relatively large-scale and slow-motion processes.



Fig. 7: Jülich sugar refinery, 01/02/2010, 11.22 Uhr (30 sec. time difference)
temperature 0°C, wind 230 °/4-7 m/s (contrast improved)

4.2 Difference of laminar / turbulent flow profiles

In respect of the change-over from the laminar to the turbulent flow pattern, Eq. 19 states that the “friction” becomes greater by a factor of 27. The flow profile at the locus of change-over has to become significantly flatter than before because of the minimum-dissipation condition.

The following conditions have to be satisfied for a change-over from laminar to turbulent flow:

Condition 1: Minimum property of local dissipation

$$\dot{E}_{lam} > \dot{E}_{turb} \quad (23)$$

according to Eq. 8

$$\mu \left(\frac{du}{dy_{lam}} \right)^2 > \frac{1}{12\sqrt{3}} \rho D^2 \left(\frac{du}{dy_{turb}} \right)^3$$

Condition 2: Sufficient input of mechanical power after change-over to turbulent flow

according to Eq. 19

$$\frac{1}{12\sqrt{3}} \rho D^2 \left(\frac{du}{dy_{turb}} \right) > 27\mu$$

or according to Eq. 21

$$Re_{D,turb} > 555$$

Condition 3: Constant shear stress (Couette flow)

$$\begin{aligned} \tau &= const. \\ &= \frac{1}{12\sqrt{3}} \rho D^2 \left(\frac{du}{dy_{turb}} \right)^2 \end{aligned} \quad (24)$$

$$= \mu \frac{du}{dy} (y \approx 0) \text{ for the laminar layer near the wall at } y \approx 0 \quad (25)$$

Applying condition 2 in condition 1, the following holds for the locus of change-over:

$$\left(\frac{du}{dy_{lam}}\right)^2 > 27 \left(\frac{du}{dy_{turb}}\right)^2 \quad (26)$$

or

$$\frac{du}{dy_{lam}} > 5,2 \frac{du}{dy_{turb}} \quad (27)$$

For the layer $y \approx 0$ near the wall, condition 2 and condition 3 lead to

$$\tau_0 > 27\mu \frac{du}{dy_{turb}}$$

or

$$\frac{du}{dy}(y \approx 0) > 27 \frac{du}{dy_{turb}} \quad (28)$$

According to these results the flow profile at the locus of change-over from laminar to turbulent flow becomes flatter by a factor of $> \sqrt{27} \cong 5,2$ and the (laminar) profile in the immediate proximity to the wall becomes steeper by a factor of $> \sqrt{27} \cong 5,2$, thus being steeper by a factor of > 27 than at the locus of change-over.

This also means that with the increase of the slope near the wall the wall shear stress also increases by a factor of $> \sqrt{27} \cong 5,2$, and so does the entire flow resistance of the experiment.

Fig. 2 provides the experimental information for the Couette flow profile. The turbulent flow profile is by a factor of ≈ 5 flatter in the middle than the linear laminar profile (see vertical arrows).

The increase of the gradient near the wall can be estimated with a factor ≈ 4 (see horizontal arrows).

In the boundary layer at the plane plate, laminar and turbulent flow forms exist at Reynolds numbers of $2 \cdot 10^5 \dots 6 \cdot 10^5$. The wall shear stress and thus the gradient near the wall changes by a factor of 3-5.

In the pipe flow, the resistance and thus the gradient near the wall changes by a factor of 2-2.5 (the assumption of a constant shear stress across the profile does not apply to the pipe flow).

4.3 Hysteresis of the laminar-turbulent-laminar transition

In the flow experiment the change laminar-to-turbulent shows remarkable differences compared with the change turbulent-to-laminar. Due to that different characteristics we use the expressions “change-over” and “transition”. The change-over experiment starts with a low laminar flow rate. The laminar character can be maintained up to very high flow rates (Reynolds number up to $4 \cdot 10^6$ for the boundary layer and up to 50,000 for the tube flow /9/).

The turbulent-to-laminar transition experiment starts with high turbulent flow rates. Reducing the flow rates takes place with stable turbulence down to a well defined low Reynolds number, the “critical” Reynolds number ($2 \cdot 10^5$ for the boundary layer, 2,300 for the tube flow /9/).

Not only the Reynolds numbers are different in the two different types of change, but additionally the local positions in the profile, where the change begins, are different.

The stability calculations performed to date do not explain these hysteresis effects. The range is told to be due to the type of disturbing function involved and the degree of turbulence of the incident flow and is referred to as „zone of indifference“ /17/. As a result, they do not consider any possible differences between a change-over from laminar to turbulent flow and a transition from turbulent to laminar flow.

L. Landau (Nobel price 1962) suggested two different critical Reynolds numbers for both types of transition. He did not investigate it in more detail “because currently there is no evidence that such cases of instability really exist” /21/.

The local Reynolds number Re_D as defined in Chap. 3 is strongly affected by the flow profile, different for laminar and turbulent flow. (The “classical” Re numbers focus on geometrical parameters like “hydraulic diameter” or “boundary layer length” etc.). The change of the profile provides some clues to an analytical approach to that hysteresis.

The transition from turbulent to laminar flow takes place at a local Reynolds number

$$Re_D < 555$$

of the turbulent zone.

The change from laminar to turbulent flow is influenced by the profile becoming flatter by a factor of $\sqrt{27}$ at the change-over point and therefore occurs at

$$\begin{aligned} Re_D &> 555 \cdot \sqrt{27} \\ &> 2888 \end{aligned}$$

of the laminar zone.

Both types of change occur at different wall distances. This condition can be formulated for the Couette flow. Assuming $\tau = \text{const.}$, $D \sim y$ ($y = \text{wall distance}$) and applying the logarithmic velocity profile, one can express the local number Re_D as a function of the shear stress for both flow patterns in different ways.

From the constant shear stress of the Couette flow and the approach according to Eq. 11 immediately results the logarithmic flow profile typical of turbulent flows.

Applying $Re_D \sim D^2 \frac{du}{dy}$ according to Eq. 20 the following holds for the turbulent flow:

$$\begin{aligned} \tau_{turb} &\sim D^2 \left(\frac{du}{dy_{turb}} \right)^2 && \text{according to Eq. 8} \\ \frac{du}{dy_{turb}} &\sim \frac{1}{y} && \text{according to Eq. 11} \end{aligned} \quad (29)$$

Consequently $Re_D \sim \tau_{turb} \cdot y$

The following holds for the laminar flow:

$$\tau_{lam} = \mu \frac{du}{dy_{lam}}$$

Consequently $Re_D \sim \tau_{lam} \cdot y^2$

The transition does not only take place at different Reynolds numbers but also at different wall distances in the flow profile. The “change-over” from laminar to turbulent flow takes place at the position where the local Reynolds number is at its possible maximum, i.e. at large wall distances. The “transition” from turbulent to laminar flow takes place at small local Reynolds numbers, i.e. small wall distances.

The distance between full turbulence and the laminar wall layer can be determined using the assumptions for the Couette flow. in Fig. 8.

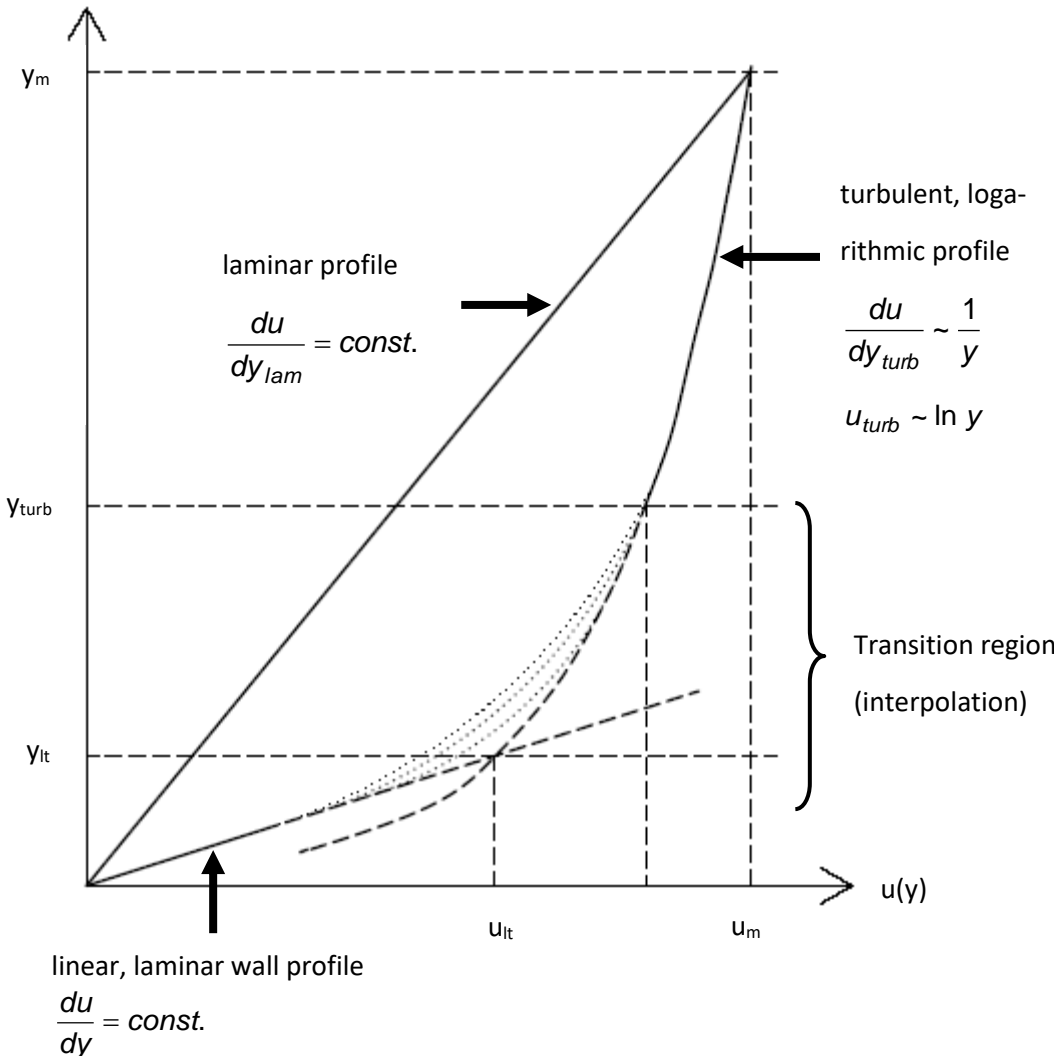


Fig. 8: Model assumption for the Couette flow

The shear stress acting in the Couette flow is constant, both in the laminar and the turbulent zone. In the proximity to the wall, the following holds:

$$\tau = \text{const.} = \tau_0 = \mu \frac{du}{dy}(y = 0) \quad (\tau_0 \text{ wall shear stress})$$

In the proximity to the wall the profile is laminar and is linear because $\tau = \text{const.}$ The gradient in the immediate proximity to the wall is well defined and measured in terms of wall shear stress τ_0 .

In the fully turbulent region $y > y_{turb}$, the logarithmic profile apply.

Empirical values /9/ have to be used and interpolated between the fully turbulent region and the linear region near the wall. A possible range is indicated with dashed lines.

For the slope of the flow profile where the fully turbulent region y_{turb} begins, and because of the constant shear stress and Eq. 19, the following holds:

$$\begin{aligned} \mu \frac{du}{dy}(y = 0) &= \frac{1}{12\sqrt{3}} \rho D^2 \left(\frac{du}{dy}(y_{turb}) \right)^2 \\ &= 27 \mu \frac{du}{dy}(y_{turb}) \end{aligned}$$

The constant slope of the laminar flow profile in the immediate proximity to the wall is reduced by a factor 27 to the beginning of the region of fully developed turbulence.

A sufficiently steep flow profile near the wall is required to introduce sufficient mechanical power into the flow for the turbulent dissipation at a greater distance from the wall. If this equilibrium is disturbed by reducing the flow velocity, the condition of turbulence for the region closest to the wall is no longer satisfied. The flow there becomes laminar. As a consequence, the laminar region near the wall becomes thicker and the turbulent flow region becomes smaller.

The discussion above allows a quantitative statement at what "classical" Reynolds number of the Couette flow the change-over from turbulent to laminar flow takes place. The size of the D-element about centre y_m extends from $y = 1/3 y_m$ to $5/3 y_m$ (y_m measured from one side of the wall). Within the size of the D-element, the gradient of the profile at y_m increases by a factor of 3 from the centre to the edge at $y = 1/3 y_m$ (and $y = 5/3 y_m$) (see Fig. 2). An average gradient

over this region, can be estimated with

$$\frac{du}{dy} \left(\frac{1}{3} y_m < y < \frac{5}{3} y_m \right) \approx \frac{2}{\sqrt{27}} \frac{u_m}{y_m}$$

and the local turbulent Re_D number in the centre according to Eq. 20

$$Re_D(\text{center}) \approx \frac{2}{\sqrt{27}} \frac{16}{9} \cdot \frac{y_m \cdot u_m}{\nu} \quad (30)$$

The “classical” Reynolds number for the Couette flow is defined /1/ as

$$Re_{\text{Couette}} = \frac{2 y_m u_m}{\nu} \quad (31)$$

$$= Re_D(\text{center}) \frac{9}{16} \sqrt{27} \quad (32)$$

Applying $Re_D < 555$

this results in

$$Re_{\text{Couette,crit}} \approx 1600$$

The critical Reynolds numbers experimentally determined, stated in the literature, range from 1200 to 1500 /9/.

We look for the inverse transition laminar-turbulent for maximum Re_D values of the laminar linear couette flow, i.e. in the middle of the channel. For that, however, the condition $Re_D > 555$. does not apply. It applies after the transition for new profile, which is flatter by a factor $\sqrt{27}$. So we can define the condition for the transition with

$$\begin{aligned} Re_{D,\text{laminar,crit}} &= Re_{D,\text{crit}} \sqrt{27} \\ &= 555 \cdot \sqrt{27} \\ &= 2888 \end{aligned} \quad (33)$$

However, this condition must not only be fulfilled in the middle of the channel at $y = y_m$, but for the area around the middle of the dimension of a D element at $y = y_m$, i.e. for $1/3 y_m < y < y_m$.

With $Re_{D,laminar,crit} = 2888$ and $y = \frac{1}{3}y_m$

$$= \frac{u_m}{y_m} \cdot \frac{16}{9} \left(\frac{1}{3}y_m\right)^2 \frac{1}{\nu}$$

with Eq. 31 follows

$$Re_{Couette,laminar,crit} \approx 29000$$

In the model calculation, too, the transition from laminar to turbulent flow form and back shows striking hysteresis effects. The laminar flow can be maintained up to very high Reynolds numbers. The turbulent flow form, in contrast, immediately changes into the laminar form when the flow falls below the so-called critical Reynolds number.

Experimental results for the Couette flow are unfortunately not known in this connection. For test conditions with particularly smooth inlet, maximum Reynolds numbers of 20,000 - 50,000 are given for the pipe flow, up to which the laminar flow could be maintained if the test was carried out carefully /9/.

4.4 Smooth local transition (“law of wall”)

In chapter 4.3 the differences during the changes laminar-to-turbulent-to-laminar are described and mentioned as “change-over” and “transition”. There is a third type of change, which has completely different features and is analyzed in the following chapter as “Smooth local transition”. There is only empirical information available in the literature, sometimes summarized as “law of wall” /9/ /20/.

In the experiment (channel, pipe, boundary layer) 100 % laminar flows can be observed, but never 100 % turbulent flows. Even with “turbulent” flows, there is always a laminar flow in the immediate vicinity of the wall at the same time. Turbulent and laminar flow forms exist simultaneously side-by-side. If the flowrate of the experiment is kept constant there is no “smooth transition”. If the flowrate is varied the “transition” takes place near and parallel the wall, in contrast to the “change-over”, which always takes place at a greater distance from the wall or in the middle of the channel.

For the discussion Fig. 9 shows empirical data of the wind profile near the ground at moderate wind speeds over a relatively smooth surface. The presentation has some similarity to Fig. 8 for the Couette flow.

Near the wall (or ground) there is a laminar layer with a steep increase of the velocity. The gradient is precisely defined and can be determined using the wall shear stress. The flat velocity profile of the turbulent flow can be seen at a greater distance. The crossed out empirical line shows the linear profile in the immediate vicinity of the wall and the logarithmic profile at greater distance with fully developed turbulence. Between them lies the so-called transition area.

We only know empirically how far this linear progression goes and when the transition area begins. There are only empirical interpolations about the transition area itself /9/.

The empirical data for different applications and experiments are summarized in the literature in a dimensionless form by using a dimensionless "shear stress speed" u_x and the "dimensionless wall distance" y^+

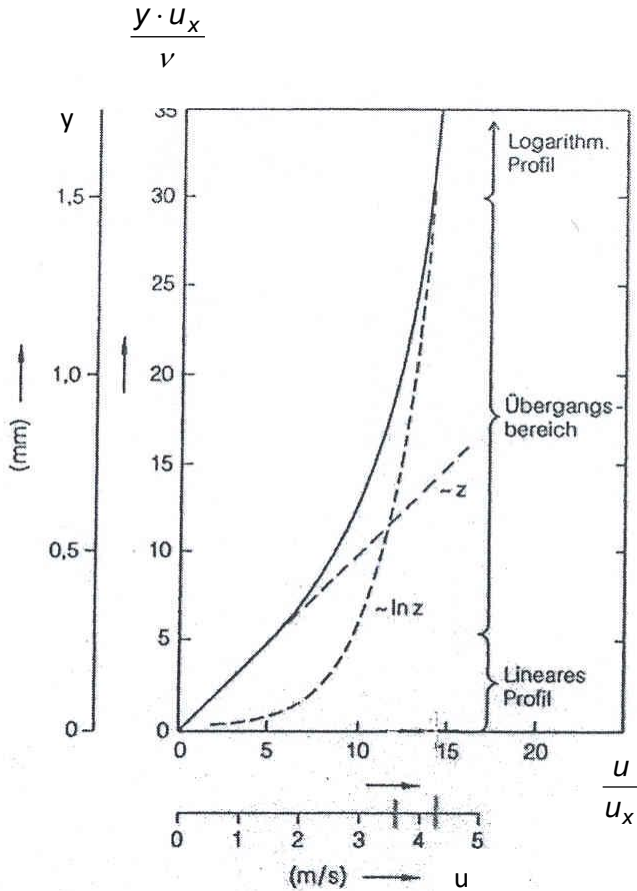


Fig. 9: Wind speed near the ground /23/

We supplement the presentation with the so-called universal "law of wall" /9/. Fig. 10 shows the dimensionless "universal" velocity profile in semi-logarithmic scaling. The logarithmic velocity distribution in the turbulent area becomes a straight line (curve 3). Curve 1 represents the linear profile close to the wall and curve 2 shows the transition range with the measured values.

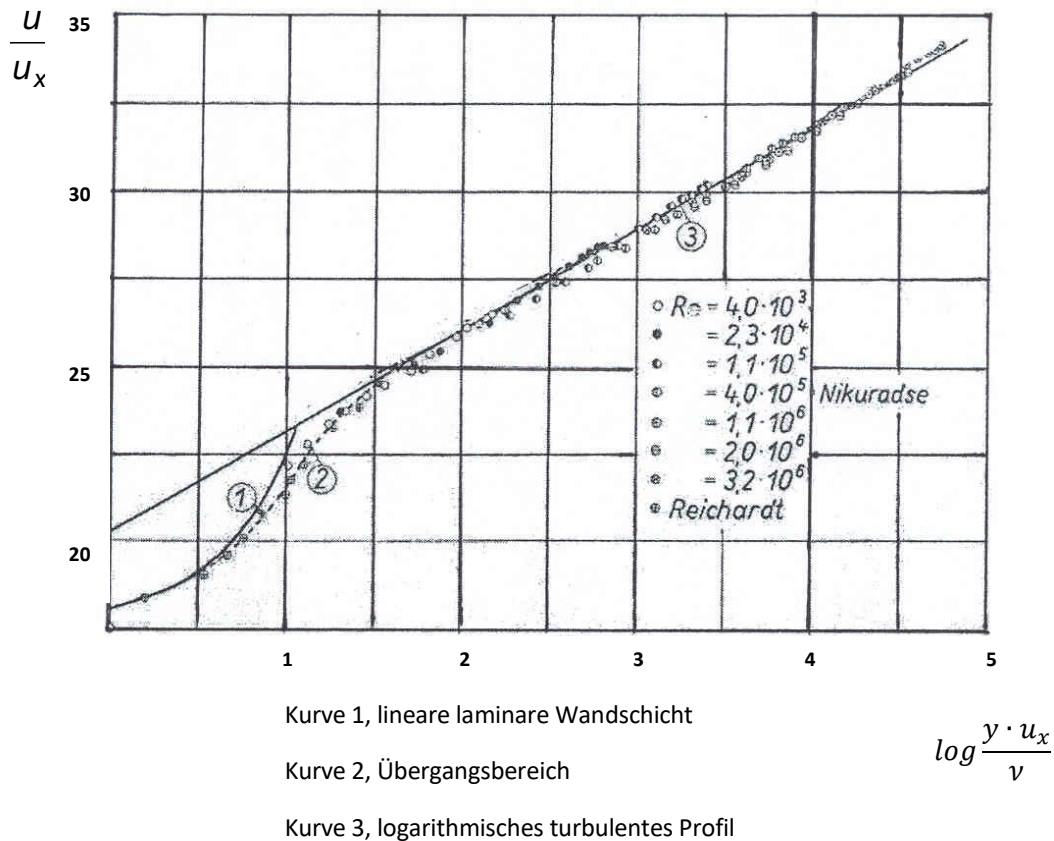


Fig. 10: Universal logarithmic velocity profile ("law of wall") /9/

How do these observations fit the model? We assume a constant shear stress, which requires a linear profile for the laminar wall boundary layer. For the beginning of the fully turbulent area, follows

$$\tau = \text{const.} = \sim y^2 \cdot \left(\frac{du}{dy}\right)^2$$

For the slope of the flow profile at the beginning of the fully turbulent range the following statements can be made.

$$\begin{aligned}\tau_{lam} &= \tau_{turb} \\ \mu \frac{du}{dy_{lam}} &= \frac{1}{12\sqrt{3}} \rho D^2 \left(\frac{du}{dy_{turb}}(y_{turb}) \right)^2 \\ &= 27 \mu \frac{du}{dy_{turb}}(y_{turb})\end{aligned}$$

or

$$\frac{du}{dy_{turb}}(y_{turb}) = \frac{1}{27} \frac{du}{dy_{lam}} \quad (34)$$

The constant gradient of the flow profile in the immediate vicinity of the wall is reduced by a factor 27 until the beginning of the area with fully developed turbulence.

We now determine the shortest distance from the wall at which the flow is just turbulent.

Condition according Eq. 20

$$Re_D = 555$$

combined with Eq. 19 results in

$$555 = \frac{\frac{1}{27} \frac{du}{dy}(y=0) D^2}{\frac{\mu}{\rho}}$$

and with $D = \frac{4}{3} y_{turb}$

$$y_{turb} = 92 \sqrt{\frac{\frac{\mu}{\rho}}{\frac{du}{dy}(y=0)}}$$

We use the so-called shear stress speed $u_x = \sqrt{\frac{\tau}{\rho}}$ to introduce the dimensionless wall distance

$y^+ = \frac{y \cdot u_x}{\frac{\mu}{\rho}}$ and obtain

$$y_{turb}^+ = \frac{y_{turb} \cdot u_x}{\frac{\mu}{\rho}} = 92 \quad (35)$$

This is the dimensionless wall distance at which turbulence is fully developed.

We compare the dimensionless wall distance 92, determined analytically in this way, with the empirical references in the literature. Rotta /24/ states a dimensionless wall distance >60 for the fully turbulent layer, Schlichting /9/ a value >70 and Prandtl /20/ a value >100 . The Newer literature mentions values $y^+ = 100$ /25/ but also $y^+ \geq 200$ /26/.

5. Numerical calculations

5.1 A 1-dimensional equation for a turbulent profile

The previous model assumptions describe the momentum exchange while maintaining the energy balance in a volume element D^3 . We apply these results to calculate the averaged flow profile in a plane shear flow (Couette flow).

Fig. 11 shows the relations. To each wall distance y there is a volume element of the dimension $D(y)$, in which a momentum exchange takes place with a defined frequency. This exchange leads to superimposed transverse flows, through which partial volumes are transported between $y + \frac{D}{2}$ and $y - \frac{D}{2}$ (the boundaries of the D-element) transversely to the main flow direction. Mathematically, this results in an “acceleration” or a “delay” to the right or left of the main flow.

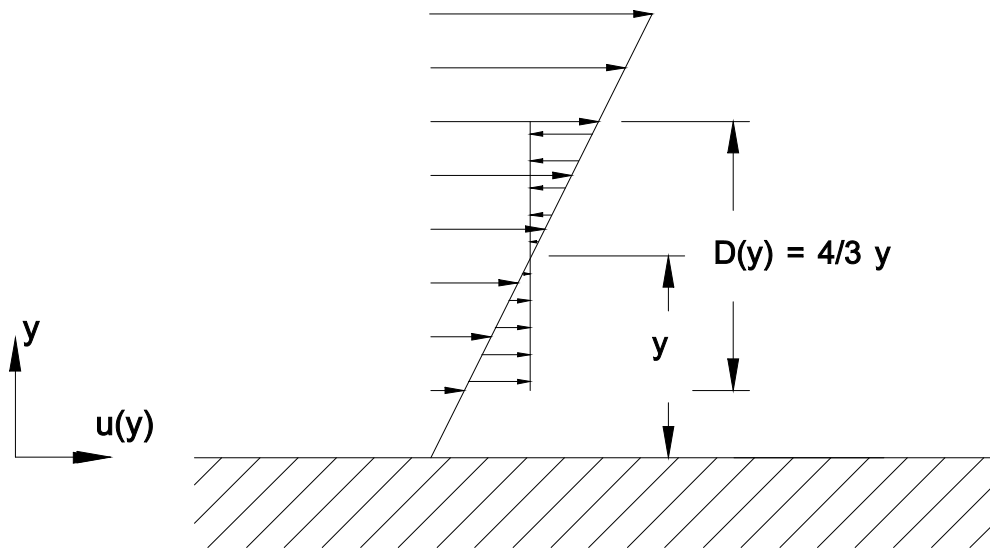


Fig. 11: Momentum exchange in the D-element

Integration over all y , to which this range relationship applies, results in the resulting total acceleration, which is zero for the mean flow values in the stationary state.

We determine the frequency of the momentum exchange in one of the many D-elements to be integrated. The maximum flow velocity is given by V_{qu} according to Eq. 7. For each of the 6 main coordinates, the mean velocity amounts $\frac{1}{6}V_{qu}$. For the profile the averaged velocity values of the two main coordinates parallel to the y -axis are effective, i.e. $\frac{1}{3}V_{qu}$.

We consider the momentum exchange in the D-element to be complete when half of the D-element is “crossed” with this velocity value. The “time” required for this is therefore

$$= \frac{D}{2} \frac{1}{\frac{1}{3} V_{qu}}$$

$$= \frac{3\sqrt{3}}{\frac{du}{dy}}$$

The frequency of the momentum exchange is the reciprocal of this

$$= \frac{\frac{du}{dy}}{3\sqrt{3}}$$

The size D is not included in this formula. It is therefore to be expected that errors or inaccuracies in the simple definition of $D(y)$ only have a minor impact on the later results in the previous chapter.

With the integration limits y_{min} and y_{max} the following equation results.

$$\frac{du}{dy}(y) = \frac{1}{y_{max} - y_{min}} \left[\int_{y_{min}}^{y_{max}} \left(\overline{u(\tilde{y})} - u(y) \right) \frac{1}{3\sqrt{3}} \frac{\overline{du}}{dy}(\tilde{y}) d\tilde{y} \right] \quad (36)$$

$$= 0$$

for stable conditions.

The values $\overline{u(\tilde{y})}$ and $\overline{\frac{du}{dy}(\tilde{y})}$ in the integral of equation 36 are not to be seen as a point value, but as an average value over the range of the D-element around \tilde{y} and are therefore marked.

Interestingly, the term “viscosity” or “shear stress” no longer appears.

The integration limits y_{max} and y_{min} result from $D = \frac{4}{3}y$, for the area near the wall with

$$y_{max} = 3y$$

$$y_{min} = \frac{3}{5}y$$

For the integration limits defined in this way, it applies that the D elements around y_{min} resp. y_{max} just reach the point y .

$$y_{max} - \frac{1}{2}D(y_{max}) = y$$

$$y_{min} + \frac{1}{2}D(y_{min}) = y$$

Fig. 12 shows the geometric relationship.

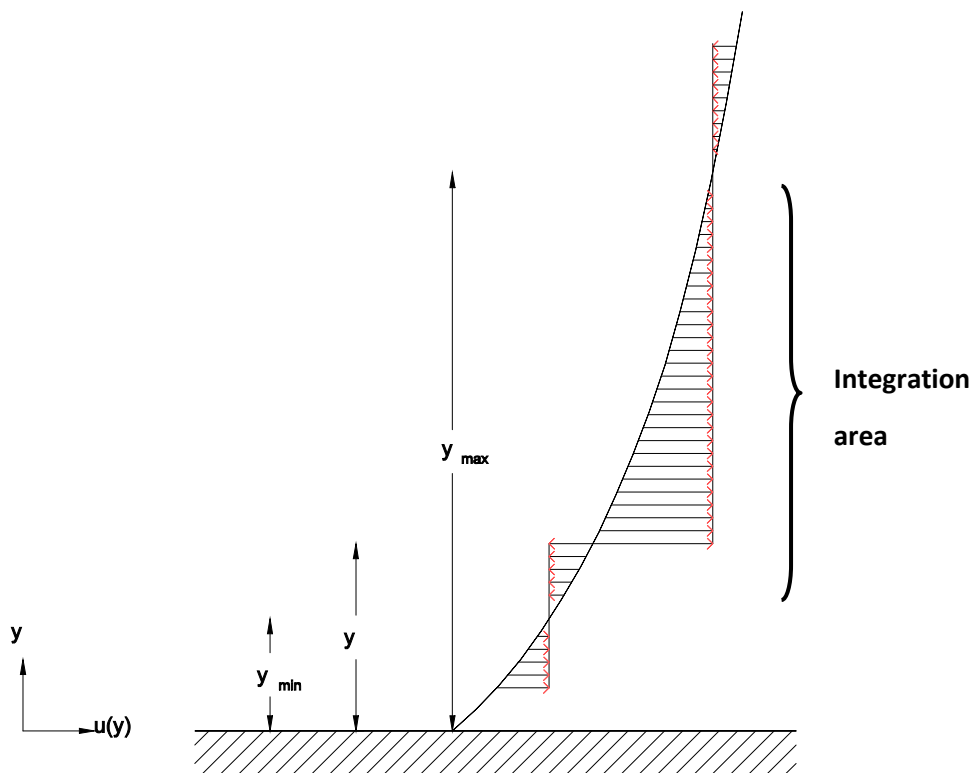


Fig. 12: Integration according to eq. 36

The integration limits defined in this way correspond to the maximum property, but do not necessarily fulfil the minimum property. This applies in particular in the vicinity of the wall, i.e. for small y and thus small y_{min} . We therefore designate with y_- the smallest wall distance for which the minimum condition 19

$$\mu_t(y_-) \geq 27\mu$$

still applies. An integration of equation 36 in the direction of the wall is thus physically permissible for

$$\begin{aligned} y_{min} &\geq y_- - \frac{1}{2}D(y) \\ &\geq \frac{1}{3}y_- \end{aligned} \tag{37}$$

The turbulent flow profile in the pipe and duct flow is calculated according to the integral eq. 36 under auxiliary conditions for the maximum and minimum values of the integration limits.

Parallel to this and especially outside the constraints, Newton's equation applies.

5.2 Numerical examples for Couette and pipe flow

The eq. 36 can only be solved analytically under simplified assumptions. We take a numerical approach, the flow profile $u(y)$ over the cross-section y is divided into a staircase function according to Fig. 13.

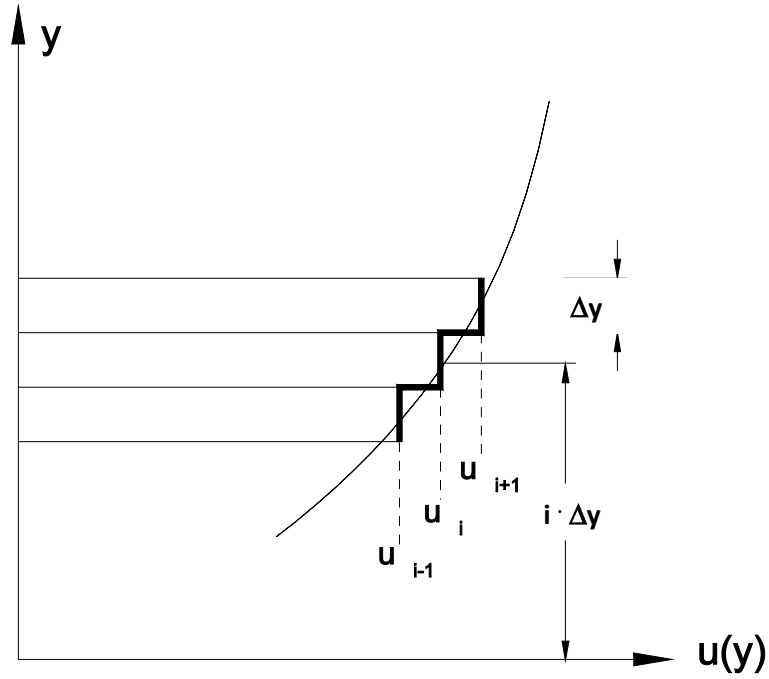


Fig. 13: Stair function for profile calculation

The step width is Δy , the respective step value u_i corresponds to the average value of u in the interval Δy around the coordinate value $y = i \Delta y$.

By analogous application of eq. 36, each u_i in each iteration step is changed by one Δu_i according to the following calculation rule.

$$\Delta u_i = \frac{1}{3\sqrt{3}(K_{max} - K_{min})} \sum_{K=K_{min}}^{K_{max}} (\overline{u_K} - u_i) \frac{\Delta u_K}{\Delta y} + \frac{\mu}{\rho} \left(\frac{u_{i+1} - u_i}{\Delta y} - \frac{u_i - u_{i-1}}{\Delta y} \right) \frac{1}{\Delta y} + \text{constant} \quad (37)$$

$\overline{u_K}$ and $\frac{\Delta u_K}{\Delta y}$ are analogous to eq. 36 numerical average values over the range $K \cdot \Delta y \pm \frac{1}{2} D(K\Delta y)$.

The summation in the first line is made for those u_K for which the turbulence conditions from eq. 19, 20 are fulfilled. The summation interval results from the definition of K_{min} and K_{max} according to the definition of eq. 36 with the constraints K_{min} and K_{max} . mentioned.

The second line considers the Newtonian laminar friction.

The step size Δu_i is limited by a selectable factor (not specified in the above calculation rule).

Furthermore, the calculated values $u_i + \Delta u_i$ must be normalized to the total flow rate $\sum u_i = \text{const.}$ after each calculation run (except for the Couette flow). For this purpose, the quantity “constant” in the third line is used, which is determined after each calculation and added to the newly set values u_i (“constant” corresponds to the element $-\frac{dp}{dx}$). The normalization is therefore part of the calculation (not with the Couette flow, since here $\frac{dp}{dx} = 0$).

The numerical results in Fig. 14 show the recalculation of the two empirical turbulent profiles in Fig. 13.

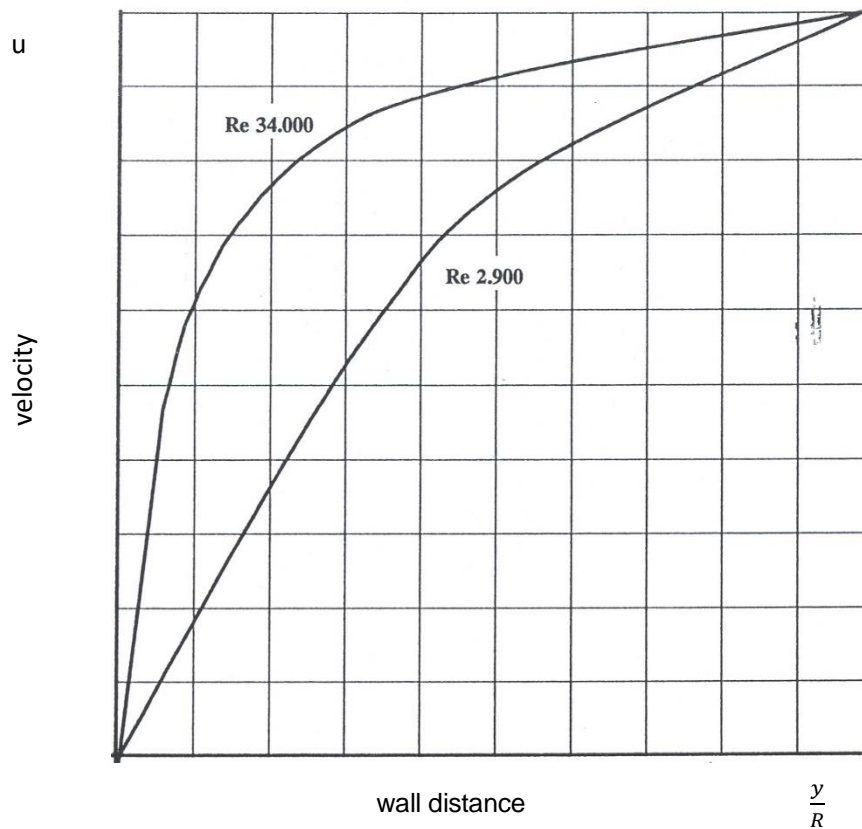


Fig. 14: Numerical calculations for the turbulent Couette flow

Fig. 15 shows the calculations for the Reynolds numbers 4000, 25000, 10^5 and 10^6 . For the values in the area of the first support point, the already mentioned limitations apply, especially for the two large Re numbers. All curves show finite gradients near the wall.

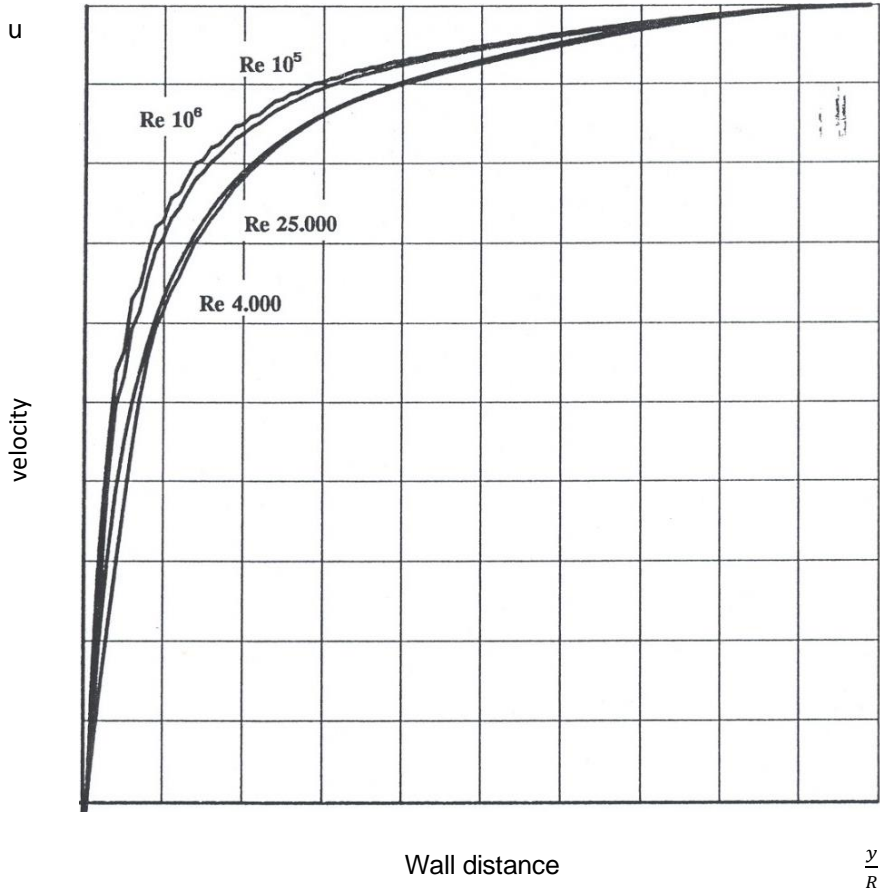


Fig. 15: Numerical calculations for the pipe flow

Infinitely high gradients near the wall are not applicable there but are often found in the literature. The gradient can be clearly determined using the flow resistance values for the pipe flow.

This is known to classical fluid mechanics and is formulated in the so-called “law of wall” correctly /9/ (see Chapter 4.4).

6. Summary

The physical principle of minimum entropy production/minimum dissipation is applied to the Couette flow to characterize laminar and turbulent behavior, the transition and the coexistence at a common boundary.

The Couette flow is the only flow form with a constant shear stress over the complete flow profile, being laminar, turbulent or both. The local dissipation defines quantitative and stable criteria for the transition laminar to turbulent and vice versa, but also for the coexistence of both flow forms.

The minimum dissipation condition leads immediately to the result that turbulent structures reach maximum macroscopic dimensions.

With the transition to and from turbulence the flow profiles change by a theoretical factor $\cong 5$ due to an increase of the “apparent” turbulent viscosity by a theoretical factor $\cong 27$. The resulting difference of the laminar and turbulent flow profiles leads to a quantitative difference of the character of the transition laminar-to-turbulent and turbulent-to-laminar. This results in two different Reynolds numbers (one for the laminar and one for the turbulent flow) and different loci of transition, which are identified by calculation.

The minimum condition results in the definition of a “local Reynolds number” which includes the local gradient of the flow profile.

The transition is a stable process. The transition to turbulence (at constant Reynolds number) requires a remarkable active increase of the input of mechanical power into the experiment – contradicting any “instability”.

A further result is associated with the special character of the Couette flow: For the experimental turbulent Couette flow profiles there is no solution possible which is based on the Navier Stokes equations.

7. Acknowledgments

The author received a personal very important comment on the first draft of that theory from his former high school teachers J. Meixner and R. Schulten, Aachen, shortly before their death. He thanks C. Buchal, D. Richter and K. Urban, Jülich, for precisely discussing the physics of the statements and the results, C.E.A. Meier and U. Nehring, Göttingen, for their important and helpful hints, their experienced judgement, also identifying doubts and difficulties and F. Durst, Erlangen for his straight remarks on what is important and what is not.

Literature

- /1/ Encyclopaedia Britannica, 15 Edition, Vol. 28, 641-645
- /2/ J. Meixner, Die Thermodynamik irreversibler Prozesse, 1960, Physikalische Blätter – Wiley Online Library
- /3/ K. Wiegardt, Theoretische Strömungslehre, Stuttgart 1965, 145
- /4/ I. Prigogine, Introduction to thermodynamics of irreversible processes, 3. Auflage, 1967
- /5/ Brockhaus Enzyklopädie, 17. Auflage, Bd. 15, 1972, 137
- /6/ S.R. de Groot, The scientific work of J. Meixner, Festschrift zum 70. Geburtstag, 24.04.1978
- /7/ W.V.R. Malkus, Outline of a theory of turbulent shear flow, J. Fluid Mech. 1, (1956) 521
F. H. Busse, Bounds for turbulent shear flow, J. Fluid Mech., vol. 41, part 1, (1970), 219-240
- /8/ Yu. L. Klimontovich, Kh. Engel-Kherbert, Average steady Couette and Poiseuille turbulent flows in an incompressible fluid, Sov. Phys. Tech. Phys. 29 (3), March 1984
Yu. L. Klimontovich, Entropy and entropy production in laminar and turbulent flows, Sov. Tech. Phys. Lett. 10 (1), January 1984
- /9/ H. Schlichting, Grenzschichttheorie, 8. Auflage, Braun, Karlsruhe 1982
- /10/ F. Durst, Grundlagen der Strömungsmechanik, Springer, Berlin, 2006
- /11/ L. D. Landau, E.M. Lifschütz, Lehrbuch der theoretischen Physik, Bd. 1, Mechanik, Berlin 1967
- /12/ A. Budó, Theoretische Mechanik, Berlin 1965
- /13/ G.E.A. Meier, Kinematische und dynamische Prozesse bei instationären Strömungen, IB 223-94A01, Göttingen 1994
- /14/ U. Nehring, Eine Impulsdarstellung kompressibler Strömungen, Z. Flugwiss. Weltraumforschung (1993) 257-269

- /15/ A. Sommerfeld, Thermodynamik und Statistik, Leipzig 1965
- /16/ Ph. R. Spalart, Philosophies and fallacies in turbulence modeling, Boeing Commercial Airplanes, P.O. Box 3707, Seattle 98124, USA
- /17/ H. Schlichting, K. Gersten, Grenzschichttheorie, 10. Auflage, Springer, Berlin 2006
- /18/ G.E.A. Meier, Göttingen, Personal statement
- /19/ Th. v. Kármán, Die Wirbelstrasse, Hamburg, 1968
- /20/ L. Prandtl – Führer durch die Strömungslehre, 13 Auflage, 2012, Springer
- /21/ L. D. Landau, E.M. Lifschitz, Lehrbuch der theoretischen Physik, Bd. 6, Hydrodynamik, Berlin 1966, 120
- /22/ I. Marusic, B. J. McKeon, P.A. Monkewitz, H. M. Nagib, A.J. Smits, K.R. Sreenivasan, Wall-bounded turbulent flows at high Reynolds numbers: Recent advances and key issues, Physics of Fluids 22 (2010)
- /23/ W. Roedel, Physik unserer Umwelt - Die Atmosphäre, 3. Auflage, Springer, Heidelberg 2000
- /24/ J.C. Rotta, Turbulente Strömungen, Stuttgart 1972
- /25/ P. Schlatter R. Örlü, Q.Li, G. Brethouwer, J.H.M. Fransson, A.V. Johansson, P.H. Alfredsson, D.S. Henningson, Turbulent boundary layers up to $Re=2500$ studied through simulation and experiment, Physics of Fluids 21 (2009)
- /26/ H.S. Dou, B.Ch. Khoo, K. S. Yeo, Instability of Taylor-Couette flow between concentric rotating cylinders, International Journal of Thermal Sciences 47 (2008)
- /27/ H. Reichardt, Gesetzmäßigkeiten der gradlinigen turbulenten Couette Strömung, Mitt. Nr. 22 des Max-Planck-Instituts für Strömungsforschung, 1959

Special parameters

τ	shear stress
τ_t	turbulent shear stress
\dot{E}	local dissipation
μ	dynamic viscosity
μ_t	apparent “turbulent” viscosity
ρ	density
l	Prandtl’s mixing length
u	speed
\bar{u}	average speed
u'	speed fluctuation
u_x	so-called shear stress speed (dimensionless)
y	wall distance
y^+	so-called dimensionless wall distance